

Predicted Solution Structure of Zymogen Human Coagulation FVII

LALITH PERERA,¹ THOMAS A. DARDEN,² LEE G. PEDERSEN^{1,2}

¹Department of Chemistry, University of North Carolina, Chapel Hill, North Carolina 27599-3290

²National Institute of Environment Health and Sciences, Research Triangle Park, North Carolina 27709-2233

Received 2 February 2001; Accepted 31 May 2001

Abstract: A model solution structure for the complete tissue factor-free calcium ion-bound human zymogen FVII (residues 1–406) (FVII) has been constructed to study possible conformational changes associated with the activation process and tissue factor (TF) binding. The initial structure for the present model was constructed using the X-ray crystallographic structure of human coagulation FVIIa/TF complex bound with calcium ions (Banner et al., *Nature* 1996, 380, 41–46). This model was subsequently subjected to lengthy molecular dynamics simulations. The Amber force field in conjunction with the PME electrostatic summation method was employed. The estimated TF free solution structure was then compared with the currently available X-ray crystal structures of FVIIa (with or without TF, variable inhibitor bound) to estimate the restructuring of FVII due to TF binding and activation. The solution structure of the zymogen FVII in the absence of TF is predicted to be an extended domain structure similar to that of the TF-bound X-ray crystal structure. An additional extension of the serine protease (SP) domain of the zymogen above a reference lipid surface by ~ 7 Å was in agreement with experiment. Significant Gla-EGF1 and EGF1-EGF2 interdomain motions in the zymogen were observed. Carbohydrate dimers attached to Ser-52 and Ser-60 did not cause restructuring in this domain. Minimal restructuring of the SP domain is found upon inference of the zymogen from the activated form. The catalytic triad residues maintain the H-bonded network while Lys-341 occupies the S1 specific site in the zymogen.

© 2002 John Wiley & Sons, Inc. J Comput Chem 23: 35–47, 2002

Key words: structure predictions; molecular dynamics simulations; FVII; tissue factor; EGF-like domains; serine protease

Introduction

Blood coagulation involves a number of serine proteases that contain highly homologous domains. The process is driven by a cascade activation of serine proteases from inactive zymogen forms, and involves a complex network of interactions regulated by positive and negative feedback loops. In the “initiation stage” in the extrinsic pathway, circulating zymogen FVII (FVII) is exposed to membrane-bound tissue factor (TF) upon vascular injury. Events following FVII exposure to TF include the activation of FVII, formation of FVIIa/TF complex that leads to proteolytic activation of factors IX and X and formation of trace thrombin.^{1–9} Thrombin activates the intrinsic pathway cofactors FV and FVIII and ultimately leads to the generation of larger amounts of thrombin required to produce a clot.

The activation of FVII,¹⁰ a single chain zymogen converted to FVIIa by cleavage of a single peptide bond, is now recognized as a primary event that in the coagulation cascade leads to cleavage of factors X and IX.^{1, 8, 11–14} The full enzymatic potential of FVIIa requires complexation with TF in the presence of calcium ions.^{11, 15, 16} Both zymogen and activated FVII forms have simi-

lar affinities for TF binding.^{17, 18} Serine proteases (SP) including factors IXa, Xa, XIIa, and thrombin have been reported to activate FVII *in vitro*, but precisely which of these is responsible *in vivo* remains unknown. It has been reported^{19–21} that the FVIIa/TF complex may also activate FVII autocatalytically under physiological conditions.

An elevated level of FVII leads to increased risk of coronary thrombosis²² while a deficiency of FVII is associated with either variable bleeding²³ or thrombotic manifestations.²⁴ Hereditary FVII deficiency is a rare, autosomal recessive bleeding disorder.^{4, 24–28} Results of this deficiency can vary from mild mucous membrane bleeding, menorrhagia, postsurgical bleeding to more severe hemarthroses, soft tissue bleeds, gastrointestinal, and central nervous system bleeding.⁴

A mature secreted zymogen of FVII is a single-chain peptide with 406 amino acid residues. Upon activation, the light chain [consisting of a γ -carboxyglutamic acid containing (Gla) domain

Correspondence to: L. G. Pedersen; e-mail: Lee_Pedersen@unc.edu

Contract/grant sponsor: NIH; contract/grant number: HL-06350 (to L.G.P.)

and two epidermal growth factor-like (EGF) domains] is covalently connected to the heavy chain (the SP domain) by a single disulfide bond. FVII is structurally and functionally related to other vitamin K-dependent (VKD) coagulation factors IX, X, prothrombin, and protein C.^{29, 30} In most of these homologous VKD serine proteases, an activation peptide is located between the light and heavy chains. During activation, the activation peptide is removed. However, no leaving activation peptide exists in FVII. The single cleavage of the bond between Arg-152 and Ile-153 yields the two-chain, disulfide bonded FVIIa.¹⁰ To investigate its activation process at the molecular level, one might require the structure of the zymogen FVII that is not currently available. Our current work is an attempt to provide an estimated zymogen structure in its solvated calcium-bound TF-free form.

Several X-ray crystal structures of the FVIIa are available.^{31–38} Although they contain a wealth of information about FVIIa, different conditions such as the presence/absence of the TF and active site inhibition from binding of different inhibitors can be found in these structures. Therefore, one must proceed with caution when comparing the structures. For the benefit of the reader, it is necessary to summarize various conditions used in the evaluation of reported X-ray crystal structures, because we compare our predicted zymogen structure with the available X-ray crystal structures in an attempt to extract information on the changes associated with activation. All experimental structures were inhibitor bound, and the structures in two cases were resolved without the cofactor, TF. Only Banner et al.³³ (pdb entry, 1dan) reported the full-length FVIIa in the presence of TF and calcium ions. However, the X-ray intensities were not sufficient to resolve the structure for the light-chain C-terminal residues 143–152. A short inhibitor, D-Phe-L-Phe-Arg chloromethyl ketone (dFFRCMK), was bound to FVIIa at the active site. The X-ray crystal structure of Zhang et al.³⁸ (pdb entry, 1fak) also contained TF and calcium ions, but the Gla domain residues 1–35 were missing, and a bovine pancreatic trypsin inhibitor (BPTI) mutant peptide (5L15) was bound at the active site. Also, residues 317–319 of the SP domain did not have any intensity. This structure was similar to Banner et al.'s³³ structure, but some difference was observed near the active site due to differences in inhibitors. One of the TF-free FVIIa (the pdb entry, 1qfk, of Pike et al.³⁷) did not contain residues 1–44, and the X-ray intensities were disordered for residues 45–48, 145–152, and 315–316. Also, the light chain residues, Lys-62, Glu-77, Lys-85, and the SP domain residues Lys-199 and Arg-202 were poorly resolved beyond the β -carbon atom, and hence, final coordinates were missing from the coordinate file for these atoms beyond β -carbon. The loop-containing residues Ser-103 to Ser-111 in the EGF2 domain were disordered, and as a result, modeled in two conformations. The active site was inhibited with D-Phe-Phe-Arg chloromethyl ketone (dFFR). The other TF-free structure given in the pdb entry, 1cvf, by Kembal–Cook et al.³⁶ had Ile-91 at the N-terminus. The EGF2 domain for this structure was rotated 7.5° relative to the SP domain when compared with Banner's structure. Also, the X-ray intensities were low for flexible residues 316–318 in the SP domain. A cleavage of the Arg-315–Lys-316 bond was necessary for stable crystallization. The active site was inhibited with 1–5-dansyl-Glu-Gly-Arg-chloromethyl ketone (DEGR-CK). Minor structural changes were found for the SP domain when compared with Banner at al.'s structure. The most recent X-ray

crystal structure,³⁴ 1dva, consists of two sets of coordinates for TF bound FVIIa. The two structures differ only in the backbone positions around residues 315–320 in the SP domain. A long peptide (E-56) was bound to an exosite distinct from the active site. The structure was speculated³⁴ to be a zymogen-like form. Residues 1–41 and 143–152 were missing from the coordinate file.

Molecular dynamics (MD) simulations, successfully applied in previous studies of other coagulation proteins,^{39–42} should yield atomic level information about the solution structure of zymogen FVIIa in its TF-free form. Also, this TF-free solution structure will serve as a valuable template for predicting the structural changes associated with the formation of the FVIIa/TF complex and organizing mutational data. Previously, we reported the solution structure of the light chain of FVII in the absence of TF.⁴² In the present work, we have undertaken a molecular dynamics (MD) simulation study to estimate the calcium-bound complete solution structure of zymogen FVII. The coordinates reported in the pdb entry, 1dan, were employed to establish a template for the zymogen FVII in solution. Because our previous report contained a detailed description on the structure of the Gla and EGF1 domains, our main focus in the present work is on the structure and function in the EGF2 and SP domains. We compare and contrast the similarities and dissimilarities, which may arise from activation as well as the association with TF, for the zymogen FVII structure with FVIIa in the X-ray crystal structures. Comparison of our findings with the results from other zymogen/active serine protease pairs may help us recognize the common features associated with structural changes due to SP activation.

Computational Procedure

Potential Functions

The second generation of the Amber force field⁴³ is employed. Two modified amino acid residues are present for which carbohydrate fragments are attached to serine residues. Ser-52 has a covalently attached glucose-initiated fragment (a dimer), while Ser-60 has a fructose-initiated fragment (a dimer). Bond, angle, dihedral, and van der Waals parameters for carbohydrates were assigned from the auxiliary Amber force field.⁴⁴ Partial charges were assigned to the atoms of Ser-carbohydrate fragments after a combined 6-31G*/HF Gaussian98⁴⁵ calculation and RESP charge-fitting procedure.⁴⁶ Solvent (water) molecules were defined by the three-point charge TIP3P model.⁴⁷

Model Construction

The initial structures of the model protein zymogen FVII was derived from the crystallographic coordinates of the FVIIa/TF/Ca²⁺ complex (pdb entry, 1dan). All crystallographic water and calcium ion coordinates assigned in the X-ray crystal structure were preserved in the initial structure. A method described in our previous work⁴⁸ was implemented to initially define the location of the N-terminus of the SP domain for the zymogen. The chymotrypsin (pdb entry, 2cga)/chymotrypsinogen (pdb entry, 4cha) X-ray crystal structures were used as references. Because 10 residues in the

C-terminal region of the light chain were missing from the X-ray crystal structure, and because the N-terminus of the SP domain was embedded into the interior of the protein, homology modeling techniques were required to introduce this missing segment into the model. The segment of residues 143–152 was then introduced to the protein model using the loop search module of Sybyl 6.4 (Tripos Inc., St. Lewis, MO). Necessary hydrogen atoms were added to the X-ray crystallographic structure followed by energy minimization of the side chains using a distance-dependent dielectric function (500 steepest descent steps followed by 10,000 conjugate gradient steps).

The protein (along with the crystallographic water and calcium ions) was then solvated in a box of water molecules so that the box boundaries are at least 12.5 Å away from any protein atom. Water molecules used in the solvation of the initial model for which the oxygen or hydrogen atoms were found to be within 2.0 Å of any atom in the protein were excluded. The central simulation box contained 406 residues of complete zymogen FVII, 22,708 water molecules, and 9 calcium ions. Three chloride ions were introduced as free nonbound counterions. These ions did not coordinate with any of the protein residues at any time during the simulation. The simulation system was thus electrically neutral. The total number of atoms in the simulation box was 75,110.

Simulation Protocol

The entire initial model was subjected to a few hundred steps of constant pressure (at 1 atm) and constant temperature (10 K) MD simulation to adjust the density. The particle mesh Ewald method,⁴⁹ as implemented in Amber version 5.0,⁵⁰ was employed to accommodate long-range interaction in all of the solution simulations. The time step was 1 fs, with the nonbonded interactions updated at every step. This choice of updating nonbonded interactions and the periodical removal of the translational and rotational motions of the center of mass (at every 2.5 ps) prevent artifacts such as the observation of the “flying ice cube.”⁵¹

After the initial density adjustment procedure, the model system was energy minimized to remove any potential “hot spots” that might ultimately lead to instability of the system. Initially, only the added water molecules were energy-minimized at constant volume (5000 conjugate gradient steps), then all the water molecules were subjected to energy minimization (another 5000 conjugate gradient steps), and finally, the entire system was energy minimized (5000 conjugate gradient steps). The system was subsequently subjected to a slow heat-up procedure (during 10,000 steps, temperature was increased with a somewhat tighter coupling constant of 0.1 ps) to adjust the temperature of the system to 300 K. After 25 ps of constant volume-constant temperature simulation, the entire system was again energy minimized (10,000 conjugate gradient steps). After another similar heat-up run of 10 ps to return the temperature back to 300 K, a constant temperature–constant volume MD run was performed for 25 ps. Finally, a constant pressure–constant temperature protocol was adopted to complete 2.9 ns of dynamics. The coordinates of the predicted zymogen structure are available on request from the author (lalith_perera@unc.edu).

Results and Discussion

Five different X-ray crystal structures^{31–38} were available to us for FVIIa in its inhibitor-bound form. These structures are valuable for obtaining molecular details of the activated SP in the presence/absence of TF and with different inhibitors bound to the active site (or exosite). Using the present model, we seek to elucidate the properties of the calcium-bound zymogen form of complete FVII, in the absence of TF or inhibitors. Because the TF bound X-ray structure of Banner et al.³³ was used to create our initial model, and because this is the only structure in which the X-ray intensities were found for all FVIIa residues (with the exception of residues 143–152 in the C-terminus of the light chain), we employ this structure as the primary reference for the majority of our structure comparisons. In the following discussion, we present a brief description of the stability of our equilibrated model system, a summary of the properties of the zymogen light chain (with a comparison to our previous simulation⁴² in which only the light chain of FVII was used), and a detailed comparison of the zymogen SP domain with that of the activated form evaluated from X-ray crystal structures. Also, we will briefly discuss the possible function of TF interactions.

Global Aspects of the Simulation and the Stability of the Model Protein

Root-mean-square deviations (RMSDs) of the backbone atoms of proteins are useful for evaluating stability and relative domain mobility for multidomain proteins. RMSDs for the zymogen were calculated with respect to the X-ray crystal configuration of Banner et al. (Fig. 1). The RMSDs calculated for individual domains

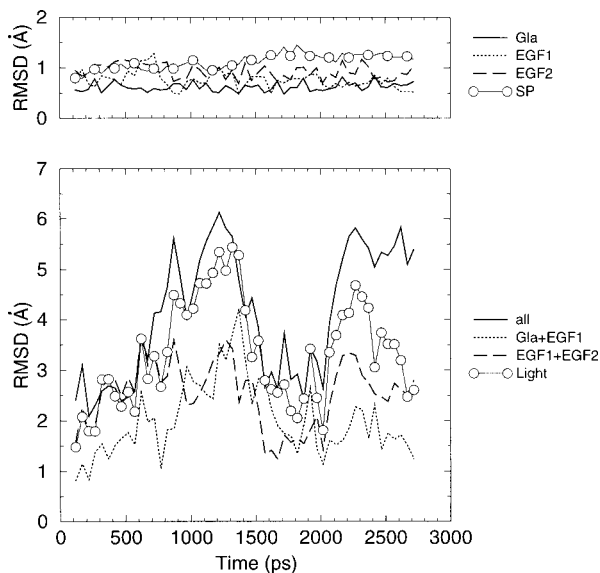


Figure 1. Root-mean-square deviations (RMSDs) of the backbone atoms, referenced to the FVIIa/TF complex of Banner et al. (ref. 33). The RMSDs of individual Gla, EGF1, EGF2, and SP domains (top). The RMSDs calculated for combined domains, Gla/EGF1 and EGF1/EGF2, the light chain and the entire protein (bottom).

(top panel) indicate highly stable domain structures (≤ 1 Å for all domains). The RMSDs calculated from the union of domains are essential for obtaining details of interdomain motion (bottom panel, Fig. 1). These combined Gla/EGF1, EGF1/EGF2 domains and the light chain or entire protein show larger magnitudes in their RMSD values than the individual domains. As has been pointed out earlier,³⁹ such deviations may arise due to relative domain motions even though individual domain structures remain relatively near those of the X-ray crystal structure. When the combined domain RMSDs are considered, the net reorganization effect is amplified. The relative magnitude of the EGF1+EGF2 combined RMSD is somewhat larger than that for Gla+EGF1, and the light-chain RMSD shows an additive effect of the RMSDs of above two combined segments. The RMSD curve calculated for the entire protein approximately follows that of the light chain, suggesting that the overall relative domain restructuring (upon activation, binding to TF) originates in the light chain. These combined domain RMSDs equilibrate with time, indicating stability of the final solution structure.

The simulation B-factors (defined by $B = [8\pi^2/3] \times \langle \Delta r^2 \rangle$ where $\langle \Delta r^2 \rangle$ is the variance), calculated for backbone atoms by averaging over the last 300-ps segment of the trajectory, are given in Figure 2. Individual domains were aligned with the $t = 0$ ps structure to remove the tumbling of the molecule in the simulation box. Such individual domain alignments also remove the effect of interdomain movements. However, this may result in larger B-factors for the residues present at the connecting regions if such interdomain motions exist, and in fact, such a signature is observed for Gla/EGF1 (near residue 46) and EGF1-EGF2 (near residue 84) domains. The general trends show that the backbone atoms in the

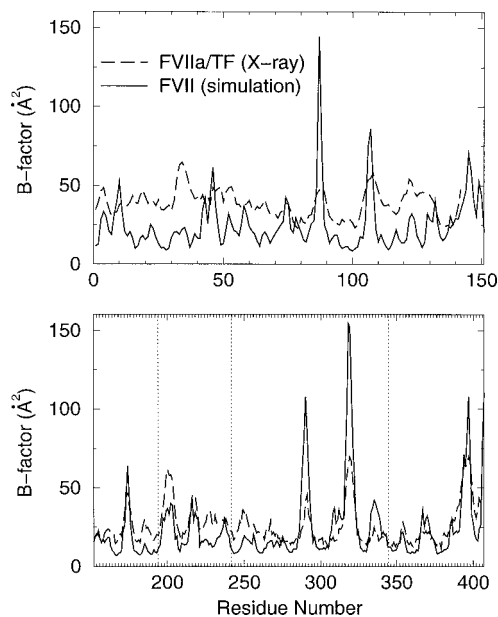


Figure 2. Experimental (FVIIa/TF of Banner et al.³³): dashed line and calculated zymogen FVII solution: solid line, B-factors of backbone α -carbons. The light chain (top); The SP domain (bottom). The catalytic residues are indicated by dashed vertical lines.

TF-free solution structure are relatively stabilized around their average positions, and the relative fluctuations around the average positions are 1–2 Å. In the light chain, the residues, in addition to those in the connecting region, that exhibit significantly larger movements, are found near Gly-107. This residue is in a turn of a beta-sheet. For the SP domain, larger B-factors are generally associated with residues in solvent-exposed loop segments and the peak positions correlate with those in the X-ray crystal structure.

We employed the program, Procheck⁵² to evaluate the “goodness” of the geometrical entities such as bonds, angles, and dihedral angles in the final TF-free solution zymogen structure. The Procheck summary showed no major discrepancies for any bond, angle, or dihedral angle in the final zymogen structure.

The Light Chain

We previously reported results from a simulation that involved only the light chain of FVIIa.⁴² We found that the light chain of FVIIa, in the absence of TF, is in an extended conformation similar to the X-ray crystal structure of TF-bound FVIIa. The removal of the calcium ion bound to the EGF1 domain led to only minor structural changes within the EGF1 domain, but resulted in a substantial relative reorientation of the Gla-EGF1 domains. General structural features observed for the light chain of the current zymogen model are also similar to those reported in our previous work on the light-chain simulation. Therefore, in this article, we will summarize only results on the features that are essential for the function of this chain. In addition, we will compare individual domain structures with the available X-ray crystal structures.

The Gla Domain

The Gla domain and the following hydrophobic stack have been shown to be important for the optimal interaction between FVIIa and TF.⁶ Likewise, it has been suggested that this fragment is important for macromolecular substrate recognition.⁵³ The Gla domain of FVII contains 10 Gla residues. Of the nine calcium ions found in the X-ray crystal structure of TF-bound FVIIa, seven are present in the Gla domain. The participation of the calcium ions in the Gla-calcium network and the N-terminal chelation complex to form the ω -loop show the same characteristics as previously reported.⁴² No H-bonds are found between the Gla domain and other domains. Comparison of the backbone C_α deviations (Fig. 3a) for this domain indicates that the overall domain structure is globally similar to the X-ray crystal structure of Banner et al.³³

EGF1 Domain

For the EGF1 domain, several X-ray crystal structures are available for comparison. The C_α deviations are presented for the zymogen referenced to the available X-ray crystal structures (Fig. 3b). Also, to assess the variation of existing experimental data, we calculated C_α deviations for the other two X-ray crystal structures using Banner et al.’s X-ray crystal structure³³ (pdb entry 1dan) as reference (Fig. 3c). The deviations (Figs. 3b and 3c) are relatively small with the backbone C_α ’s of Ala-51, Ser-52 (O-glycosidically bound to a carbohydrate,^{54–56} and several residues in the EGF2 connecting region showing deviations larger than 1 Å. It thus appears that the interaction with TF does not introduce appreciable restructuring. In fact, side chains of the TF binding residues have

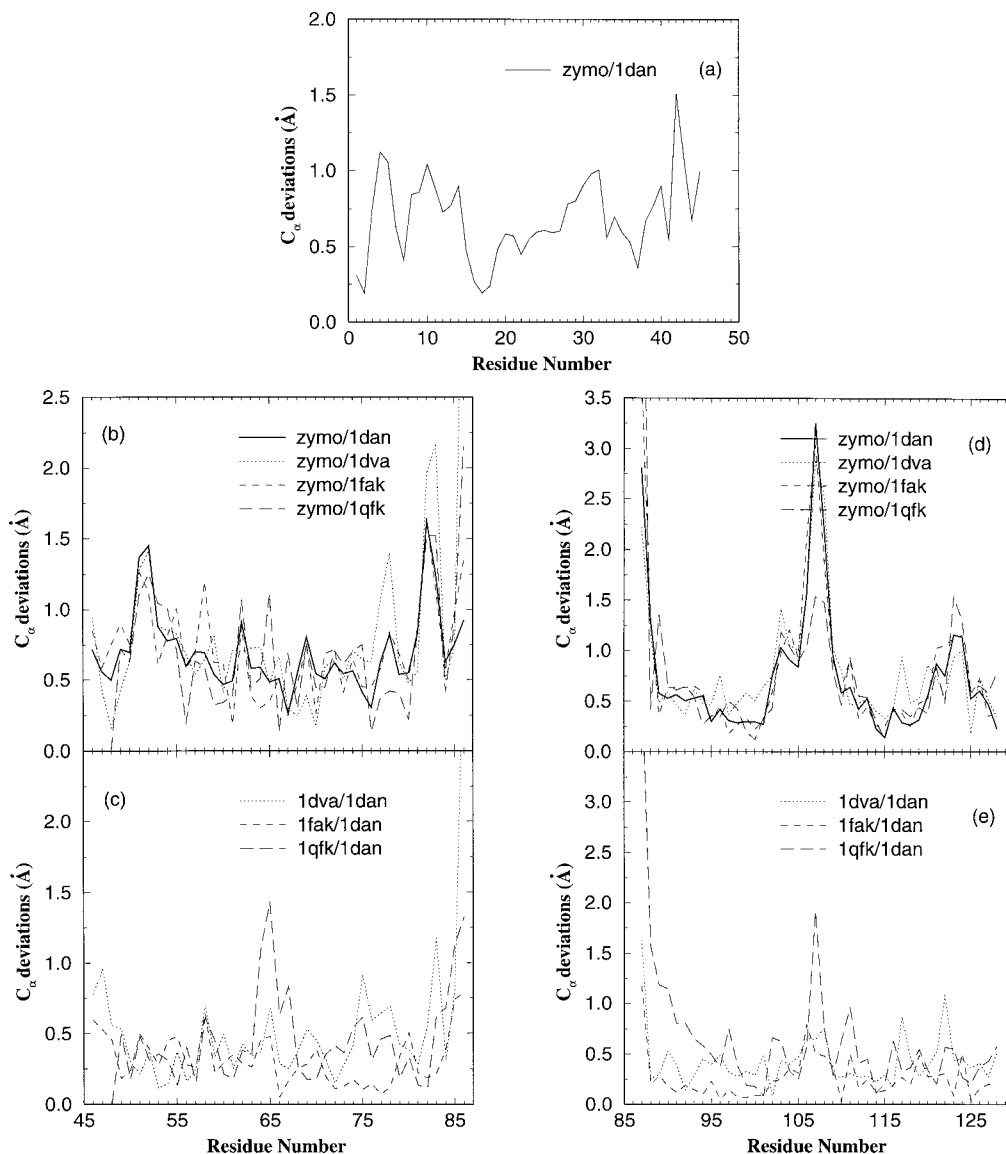


Figure 3. Deviations of the α -carbon atoms of the zymogen and available X-ray crystal structures. (a) The Gla domain; (b) the EGF1 domain of the zymogen solution structure is compared with all available EGF1 X-ray crystal structures; (c) EGF1 domains of other X-ray crystal structures are compared with the X-ray crystal structure of Banner et al.³³; (d) the EGF2 domain of the zymogen is compared with all available EGF2 X-ray crystal structures; (e) EGF2 domains of other X-ray crystal structures are compared with the X-ray crystal structure of Banner et al.³³

comparatively large solvent accessible areas and relatively large B-factors (data not shown), indicating that side chain adjustments may be sufficient to introduce TF binding to this domain.

The EGF1 domain of FVII has unique carbohydrate moieties O-glycosidically linked to two serine residues (Ser-52 and Ser-60).^{54–56} These attachments are believed to provide unique structural elements required for rapid association of FVII or FVIIa with cellular receptors and cofactors.⁵⁵ The direct biological function of the carbohydrate attachment is as yet unknown, although mutations at Ser-52 and Ser-60 (by Ala) show reduced clotting

activity for FVIIa.⁵⁵ Iino et al.⁵⁵ found indistinguishable changes in TF-dependent and independent amidolytic activity for mutants compared to the wild type. In our previous simulation of the light chain of FVIIa, the carbohydrate functionality was absent. However, in the present study, the carbohydrates are modeled as O-glucosidically-linked dimers to Ser-52 and Ser-60. These carbohydrates are solvent exposed and do not significantly alter the structure of this domain (see RMSDs in Fig. 1 and C_α deviations in Fig. 3b). In fact, the NMR experiments on the EGF1 domain by Kao et al.⁵⁶ led to the conclusion that the overall structure of

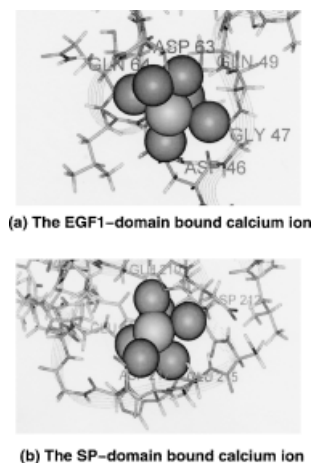


Figure 4. Coordinations of (a) the EGF1 domain-bound calcium ion and (b) the SP-domain bound calcium ion in the predicted zymogen structure. Water molecules that are coordinated with calcium ions are omitted from the display.

glycosylated FVII EGF1 is similar to the nonglycosylated form even for the residues near the glycosylation sites. Ser-52 does not form H-bonds with other residues in this domain, but the H-bond between Ser-60 and Phe-71 found in the X-ray crystal structure³³ is preserved throughout the simulation.

It has been suggested⁵⁷ that the calcium ion in the EGF1 domain has no direct effect on contacts with TF residues, but that the overall docking of FVIIa/TF is enhanced through a Gla-EGF1 orientation stabilized by calcium binding. The calcium ion in the X-ray crystal structure of FVIIa/TF is found to be octahedrally coordinated with six oxygen ligands (Asp-46:OD2, Gly-47:O, Gln-49:OE1, Asp-63:OD1, and OD2, and Gln-64:O) (see Fig. 4a). In this “pseudo-octahedral” configuration, four corners are occupied by oxygen atoms with the fifth corner by the Asp-63 carboxylate. The sixth corner is assumed to be occupied by a water molecule, not explicit in the experimental study. In fact, two additional water molecules were accommodated in its coordination sphere in the TF-free zymogen solution structure. These water molecules remained rather immobile during the trajectory calculations. This arrangement is preserved during the entire trajectory calculation indicating strong coordination of the water molecule with the calcium ion. The removal of this calcium ion in our previous simulation of the light chain⁴² led to substantial relative orientation of the Gla and EGF1 domains. In a similar structure evaluation for zymogen factor IX, however, we observed⁵⁸ a relatively weak coordination for the corresponding calcium ion.

EGF2 Domain

Smaller RMSDs for this domain indicate relatively negligible re-orientation for this domain upon solvation. This is confirmed by the C_{α} deviation plot shown in Figure 3d. Only the residues in the EGF1 connecting region and several residues in the beta turn of the loop region of 103–111 show comparatively larger C_{α} deviations. Few residues of the EGF2 domain make direct TF contacts, and apparently all are in the segment 85–93. Interestingly, compared to the other three structures, the C_{α} deviations are small for the

zymogen/(X-ray crystal structure of the pdb entry, 1qfk) pair in the segment of residues 105–108. The X-ray crystal structure of the coordinate set (1qfk) was determined in the absence of TF. This observation suggests that the segment 105–108 may be indirectly involved in TF binding. Retention of the overall fold of this domain on solvation is not surprising, because it has been shown that the EGF-like domains of FVIIa remains stable under high guanidine hydrochloride concentrations and at elevated temperatures.⁵⁹

The mutation Gln100 → Arg in the EGF2 domain has been detected^{60–62} in 19 out of 21 severely FVII-deficient patients. Direct binding analysis of wild type and the Gln100 → Arg variant of FVII and FVIIa to soluble TF was performed by Kembal-Cook et al.⁶¹ using surface plasmon resonance. The outcome was severely reduced binding of the mutant of both FVII and FVIIa to TF. In the X-ray crystal structure, Gln-100 has two H-bonds with Asn-95 and His-115. This H-bonding network is maintained during the entire 2.9-ns simulation. In a separate study, Oming et al.⁶³ showed that a synthetic peptide derived from the region bracketing Asn-95 and Gln-100, inhibits the TF-dependent FX activation of FVIIa. They concluded that this segment has a direct role in the formation and function of the FVIIa/TF/FX complex. Also, the H-bond found between Asn-95 and the SP domain Thr-272 in the X-ray crystal configuration is preserved during the trajectory calculation of the zymogen. Thus, a possible function of TF may be to properly orient this motif for possible FX interaction.

The relatively large RMSD observed for combined EGF1-EGF2 domains can be assigned to the interdomain motion of the EGF1 and EGF2 domains via the connecting region (residues 82–90), possibly brought about by the absence of TF. Of the VKD proteins with the EGF1-EGF2 unit, FVII processes the largest number of residues in the connecting region. If the two domains individually require specific structural orientation for TF interactions, the longer length of the connecting region may possess an advantage. Aligning the EGF2 at a certain orientation with EGF1 may clamp the orientation of SP domain possibly suitable for its function, because little EGF2/SP interdomain motion is observed during the dynamics. The SP domain, hence, appears to simply sit atop the EGF2 domain.

For its function of activating FX, FVIIa requires calcium-dependent binding to membrane surfaces containing anionic phospholipids. Having a particular location of the active site from the membrane surface may be important for the function of the activated SP, because the FVIIa/TF/FX complex resides on the membrane surface. Using fluorescence energy transfer between a donor dye bound to the FVIIa active site and an acceptor dye located at the membrane surface, McCallum et al.^{64, 65} estimated the distance of the active site from the membrane surface in the presence and absence of TF. In the absence of TF, the distance to the active site from the membrane is estimated to be 82 ± 3 Å. This distance is reduced in the presence of TF so that the catalytic triad residues are approximately 6–8 Å nearer the membrane surface. For comparison, the plane containing the calcium ions bound to the Gla domain can be taken as a reference for the actual lipid surface in a physiological situation. This surface is well defined, and therefore, we can estimate the distance from this surface to the active site of FVIIa. This distance was found to be approximately 86 Å for the X-ray crystal structure of FVIIa determined by Banner et al.³³ Using the same definition, the distance mea-



Figure 5. Backbone ribbons of the X-ray crystal structure of TF-bound FVIIa (light) and the final simulated zymogen FVII (dark). Also, TF from the X-ray crystal structure and the calcium ions (in both X-ray structure and the solution structure) are shown.

sured from such hypothetical surface increased to approximately 93 Å for the final structure of the present FVII zymogen model (see Fig. 5). The observed 7 Å difference in the distance agrees with the experimental finding.^{64, 65} The agreement seen here may be fortuitous, because the experimental measurements were done only with a single donor-acceptor pair, and there may have been relative wobble of perpendicular molecules throughout the measurement time; however, it is encouraging. Further analysis of the simulated structures points to the EGF1/EGF2 connecting region as the focus of the movement of the active site towards the lipid surface induced by TF binding. The zymogen solution structure, then, is consistent with the notion that the cofactor, TF, may align the active site of FVIIa with the substrate cleavage site of FX at a specific orientation above the membrane surface.^{64, 65}

The Heavy Chain

The five available X-ray crystal coordinates^{31–38} are used for structural comparison with the current predicted solution structure of zymogen FVII. We hope this will lead to identify motifs that characterize structural changes associated with the activation process and TF binding.

From RMSDs we have observed that the restructuring of the SP domain is minimal with the relative magnitude comparable with the other domains considered individually. The B-factors calculated for the SP domain of the zymogen backbone atoms display the same oscillatory patterns as the X-ray crystal structure of the TF-bound activated FVIIa of Banner et al.³³ (see Fig. 2). This is not surprising, because all of the prominent peaks found in the plot can be ascribed to surface loops of the SP domain. However, the B-factors of the side chains are more drastically fluctuating for these surface loops when compared with X-ray crystal structure counterpart (see Fig. 6). In fact, we can observe a relatively

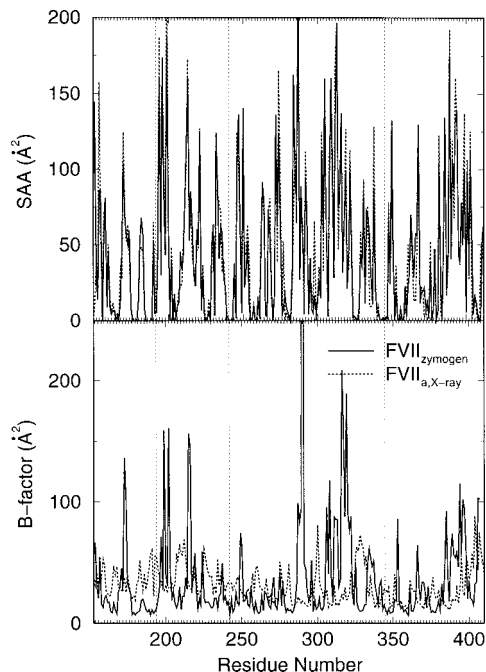


Figure 6. Side-chain B-factors (bottom) averaged over the heavy atoms of side chains of each residue of the catalytic domain of the zymogen FVII (solid line) are compared with those of FVIIa (X-ray crystal structure of Banner et al.³³). Solvent-accessible areas are also included (top). The positions of the catalytic residues are indicated by vertical dotted lines.

strong correlation of the B-factors and the solvent accessibilities (calculated using the program, Naccess⁶⁶) in the figure (top panel) for this domain while almost no correlation with the B-factors of the X-ray crystal structure of Banner et al.³³ Relatively high B-factors (and surfaces accessibilities) were observed in the segment of the residues 287–294 (cn144–152). This segment has been implicated in factor X binding.^{67, 68} The residues involved in TF binding [segment 304–308 (cn162–166)] and the adjacent segment that contains missing or mobile residue segments [residues 316–319 (cn170D–170G)] observed in different X-ray crystal coordinates files also have large B-factors and solvent accessibilities in their side chains. Arg-315(cn170C) forms H-bonds with residues Val-371(cn222) and Gly-372(cn223) and its side-chain B-factor and solvent accessibility are found to be relatively small compared with its neighboring residues. Removal of the crystal packing (crystal → solution), removal of TF, and solvation effects contribute to the above differences.

As described in our work of modeling zymogen protein C,⁴⁸ much longer simulation times may be required for sampling all of the transitions that may take place in the refolding (FVIIa crystal → FVII zymogen solution). Based on other zymogen/activated SP pair studies, one such transition that we are relatively confident must occur is that of the rotation of the carboxylate group and amido nitrogen of Asp-343(cn194) [the residue adjacent to the catalytic Ser-344(cn195)]. This transition was found to develop slowly in the initial segment of the simulation (during the first 1.5 ns). By employing constrained dynamics, the reverse

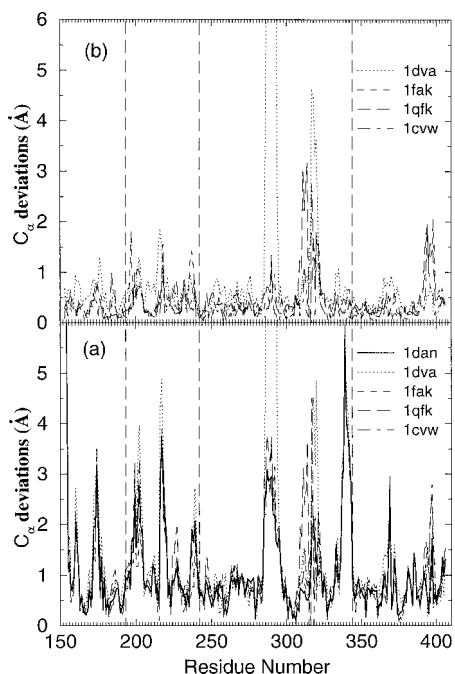


Figure 7. (a) Deviations of the α -carbon atoms of the corresponding residues of FVII in the zymogen solution form and the activated forms found in X-ray crystal structures after the optimal alignments. Pdb entries, 1qfk and 1cvw, were X-ray crystal structures of TF-free FVIIa while 1dva involves an exosite bound protein. (b) All other X-ray crystal structures are compared with Banner et al.'s³³ structure. The position of the catalytic residues are indicated by vertical dotted lines.

transition process was accelerated during the 1.5–1.6 ns time interval. The dynamics after 1.6 ns was subsequently relieved of constraints. The final structure of the simulation is then assumed to be reasonably nearer to what one may find in native zymogen FVII.

To ascertain the structural changes that may be associated with the activation of FVII, we examine the differences found in the local structure of the zymogen backbone when compared with the inhibitor-bound activated FVII. In Figure 7a, C_{α} deviations of the available X-ray crystal structures of FVIIa SP domains are compared with the solvent-equilibrated zymogen after maximal superposition. Also, to establish the spread of C_{α} deviations among experimental structures the other X-ray crystal structures are compared (Fig. 7b) with the Banner et al.³³ structure, because it was used as the initial template for the model building of the zymogen.

In the comparison of X-ray structures among themselves (Fig. 7b) we find few prominent peaks. The most striking is the peak near the residues 285–294 (cn142–152) for the X-ray structure given in pdb entry, 1dva. Mutations of this loop affect the activation of FX.^{3,67,68} The X-ray crystal structure given in the pdb entry, 1dva, was resolved³⁴ with the presence of TF and a long peptide that could bind to an exosite (around the residues in a trough that is distinct from, but near the active site; one wall of this trough contains the SP domain calcium ion binding site) on the SP domain of FVIIa. This peptide noncompetitively inhibits activation of FX and amidolytic activity. Dennis et al.³⁴ have suggested that the loss of the Gln-286(cn143) and Lys-341(cn192)

H-bond occurred due to the above loop movement. Lys-341(cn191) is near the amide N of Gly-343(cn193) and the amide N of Ser-344(cn195) that participates in the formation of the oxy-anion hole. Indeed, in the predicted zymogen solution structure this loop is disordered (deviates from experimental structures), as the above H-bond is absent. In the zymogen structure, Lys-341(cn191) is located so that it occupies the S1 site of FVII. Thus, it appears reasonable that a change in this loop conformation is necessary for FVII to reach its activated form. In fact, Dennis et al.³⁴ proposed that the peptide (E-56)-bound structure may induce a zymogen or zymogen-like structure that results in the inhibition of FVIIa's activation of factor X. Pike et al.³⁷ observed amplified movement of the surface-exposed α -helical segment near residues 307–312 (cn165–170). In the Banner et al.³³ X-ray crystal structure Met-306(cn164) is sandwiched in a hydrophobic groove on the surface of TF with several side chains of TF residues capping this helix. Pike et al.³⁷ hypothesized that stabilization of this loop is a prerequisite for the proper formation of the activation domain. However, this segment is not found to be displaced from the orientation of Banner et al. in either our zymogen solution model or the X-ray crystal structure of the pdb entry, 1dva. The disorder found in the adjacent region of residues 315–318 (cn170C–170F) in the X-ray crystal structures is due to either missing residues in this region or to poor X-ray intensities. In fact, most of other C_{α} deviations [except those that occur near residues 338–343 (cn189–194)] are due to the movements associated with surface-exposed loops. The segment 338–343 (cn189–194) displays characteristic backbone movements associated with the activation process.

Comparison with Other Zymogen/Activation Form Pairs

C_{α} deviations of three SP systems for which both the active and zymogen X-ray crystal structures are available can be compared with the C_{α} deviations of zymogen vs. the X-ray crystal structure of FVIIa of Banner et al.³³ This comparison should assist in identifying common features that may be ascribed to the activation process. In Figure 8, we compare the FVII system with chymotrypsin (pdb entry, 2cga)/chymotrypsinogen (pdb entry, 4cha), α -thrombin (pdb entry, 1hah)/prethrombin 2 (pdb entry, 1hag) and porcine pancreatic elastase (pdb entry, 1btu)/bovine proproteinase E (pdb entry, 1pyt) protease active form/zymogen pairs. Note that we use the chymotrypsin numbering (cn) system to facilitate the comparison. Once superimposed, the catalytic triad residues are essentially indistinguishable for zymogen and activated SP pairs; i.e., they superimpose closely. The two prominent peaks around residues 285–296 (cn142–154) and 334–343 (cn186–194) are characteristic features of the transition from zymogen to active form. Although in the previously modeled zymogen/activated pairs for FIX⁵⁸ and protein C⁴⁸ we observed the same signature of activation, the C_{α} deviations peak around residues 285–296 (cn142–154) for both those systems were found to have the same magnitude as the experimental X-ray crystal structures. In fact, there is a significant influence from the N-terminal region of the SP domain on the structure of this loop, due to significant structural changes associated with the N-terminus upon activation. Other proteins homologous to FVII in the coagulation cascade contain an activation peptide that connects the light chain with the SP domain, but is removed at ac-

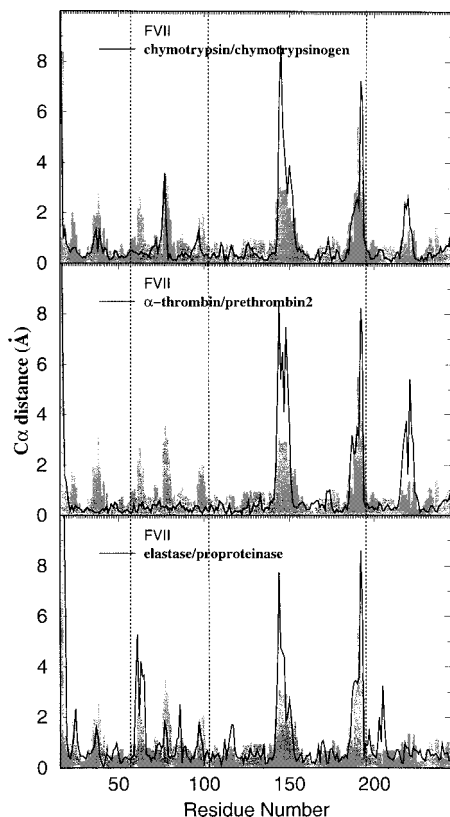


Figure 8. Comparison of C_{α} deviations of FVII (active vs. zymogen: same shaded histogram in all three panels) and (top) chymotrypsin/chymotrypsinogen; (middle) α -thrombin/prethrombin 2 and (bottom) elastase/proproteinase. The chymotrypsin numbering is employed for comparison. The positions of the catalytic residues are indicated with vertical dashed lines.

tivation. FVII does not contain such an excised activation peptide, and this may affect the structural transitions associated with loop 285–296 (cn142–154). It is reasonable to assume that other smaller peaks in the C_{α} deviation plot that are not common for the SP pairs may contribute to the specificity of the activated SP.

It is intriguing to study the conserved H-bonded network for the catalytic triad residues in the zymogen form. Indeed, in the predicted zymogen His-193(cn57) bound to Asp-242(cn102) more strongly than for the X-ray crystal structure. This H-bonded network is found extended in the zymogen form to include: Asp-196(cn60), Cys-194(cn58) H bonded with His-193(cn57) and Ala-192(cn56), Ser-363(cn214) and Thr-378(cn229) H-bonded with Asp-242(cn102). Also, Lys-341(cn192) blocks the S1 specific site in the zymogen form and additionally forms a H-bond with Ser-363(cn214). The H-bond found in the activated forms between Gly-179(cn43) and Ser-344(cn195) has been preserved in the zymogen form. This extended H-bond network is evidence for a pre-formed catalytic triad in the zymogen form. Removal of steric hindrance to the formation of the substrate-specific binding sites thus appears to be major object of the activation process.

The role of Phe-374(cn225) in the cofactor-mediated, allosteric regulation of FVIIa was studied by Petrovan and Ruf.⁶⁹ Muta-

tion of Phe-374(cn225), however, did not abolish the function of FVIIa. The mutant had normal activity as a free enzyme, but when compared with the wild type, it showed reduced proteolytic and amidolytic function in the presence of TF. We found that in the zymogen this residue is relatively nearer to the S1 specific binding pocket but that the conformation is unaltered from that of FVIIa. This residue is sandwiched between two loop segments and a part [residues 310–314 (cn168–170B)] from a short helical segment that is solvent exposed. No detectable movement in the loops is observed for residues surrounding Phe-374(cn225) when the zymogen is compared with the active form. Because the conformation for Phe-374(cn225) is similar in both active and zymogen forms, because it is in close proximity to the S1 specific site, and because the segment 307–312 (cn165–170) does not significantly differ in predicted zymogen and active conformations of FVII, the suggestion (in ref. 69) of a role for Phe-374(cn225) as an allosteric regulator that transmits the activating switch from the cofactor (TF) interface to the catalytic cleft is reasonable.

Both zymogen and the active forms of FVII possess a high affinity calcium binding site in the SP domain. Using the homology considerations of FVIIa to trypsin and its calcium binding, Schieodt et al.⁷⁰ and Sabharwal et al.⁷¹ predicted the location of this site. The predicted position was later confirmed through Banner et al.'s and others X-ray crystal structures. In Banner et al.'s structure,³³ Glu210(cn70):OE1, Asp212(cn72):O, Glu215(cn75):O, and Glu220(cn80):OE2 coordinated directly with the calcium ion along with two crystallographic water molecules. Asp-217(cn77) bound to the calcium ion through a water molecule. In the pdb entry, 1fak, the coordination was similar to the above, but differs only in the coordination mentioned for Asp-217 (cn77). Both pdb entries, 1fak and 1cvw, had similar coordination for calcium as the entry, 1fak, but there were two coordinations reported from Glu-210(cn70). All these coordinations were found in the structure of the pdb entry, 1dva, but there was no mention of the presence of water molecules in the coordination shell. In the current predicted zymogen structure, we observe all of the above ligands plus two water molecules in the coordination shell (Fig. 4b, waters are not shown). According to Sabharwal et al.'s⁷¹ findings, even in the absence of this calcium ion, TF can interact with the SP domain, but the calcium binding to SP domain increases FVIIa's affinity towards TF by 10^5 . Further investigations are warranted to pinpoint the molecular nature of the function of this calcium ion.

Analysis of the electrostatic potential surface calculated using the program, Grasp⁷² (results not shown) clearly indicates that in the activated form the S1 site is highly electronegative for attracting the positively charged P1 substrate residue arginine. The neighboring environment of this site is found to be electroneutral. In the predicted zymogen form, however, the electrostatic potential is substantially less electronegative near the S1 site. Thus, as a result of the activation process, the electrostatic potential of the entire active site may change so as to accommodate the substrate cleavage.

We have recently completed a simulation study⁷³ in which TF-bound FVIIa in its native conformation and a TF-bound chimera of FVIIa (the entire EGF1 domain of FVIIa was mutated to represent that of FIX) were subjected to MD simulations to study the allosteric effect of TF interaction on the active site of FVIIa. Two surface loops [loop 1 (residues 331–337 (cn184–

188)), and *loop 2* (residues 369–374 (cn221–225))] in concert with *loop 140* (residues 285–294 (cn142–152)) and the N-terminus insertion form the so-called “activation domain” in FVIIa, which is stabilized by conversion of the zymogen to the active serine protease.⁷⁴ Also, for substrate specificity, interactions with residues on *loop 170* [residues 312–329 (cn170–182)] are important.⁷⁵ In the wild-type FVIIa/TF simulation,⁷³ stable H-bonds were reported for Ser-314(cn170B)-Gln-366(cn217), Ser333(cn185)-Gln313(cn170A), Asp-338(cn189)-Val154(17), Asp-338(cn188)-Ala369(cn221A), and Met-327(cn180)-Arg379(cn230) residue pairs, while none of the above H-bonds were observed in the simulation of chimera FVIIa/TF.⁷³ FVII is in the TF-free form in the present simulation. We find that most of H-bonds connecting *loop 1* with *loop 170* in the FVIIa/TF simulation are missing

from the current simulation system. A lone H-bond that was observed in the X-ray crystal structure between Ser-333(cn185) and Asp-372(cn223) is also found for the zymogen. Also, the strong H-bond between Asp-338(cn188) and Val-154(cn17) found in the simulation of FVIIa/TF⁷³ is not observed in the present TF-free zymogen case, perhaps due to the restructuring around the N-terminal residues. However, there is a strong H-bond between Lys-337(cn187) and Gly-155(cn18), the neighbors of the previously H-bonded residues [Asp-338(cn188) and Val-154(cn17)]. Virtually all H-bonds connecting *loop 2* with *loop 170* can be found in the TF-free form with the exception of Ser-314(cn170B)-Gln-366(cn217). The current simulation data supports the previous suggestion that the integrity and stability of the so-called “activation domain”⁷⁴ is established by TF binding.

Table 1. Point Mutations That Lead to FVII Deficiency with High Clinical Severity.

| Mutation | C _α Deviations | SA (zymo/X) | H-Bonds | Van der Waals Contacts | Position |
|--|------------------------------|----------------|--|---|----------|
| Arg247Ser (cn107) (ref. 27) | 0.36 | 34/37 | Ala-226(X) Gln-227(X) Ser-393 | Ile-186, Trp-187, Ala-226, Gln-227, Ser-393, Pro-395 | surface |
| Arg277Ser (cn134) (ref. 27) | 0.91 | 122/165 | Arg-304(X) | Pro-303, Arg-304 | surface |
| Ser282Arg (cn139) (ref. 27) | 0.89 | 9/5 | Gln-167 | Gln-167, Met-298, Val-299, Lys-346, Pro-347, Val-362 | interior |
| Ala294Val (cn152) (ref. 26) | 1.57 | 26/6 | Gly-285 Gln-176 | Gln-176, Trp-284, Gly-285 | surface |
| Pro303Thr (cn161) (ref. 27) | 0.38 | 13/18 | Gly-331(X) | Arg-277, Phe-278, Ala-330, Gly-331, Trp-332 | surface |
| Phe328Ser (cn181) (ref. 80) | 0.35 | 2/0 | Tyr-377(X) | Arg-304, His-348, Thr-359, Gly-360, Val-376, Tyr-377, Arg-379 | interior |
| His348Gln (cn199) (ref. 81) | 0.92 | 0/0 | Gly-360(X) Thr-359(X) | Ser-279, Leu-280, Val-281, Arg-304, Phe-328, Leu-358, Thr-359, Gly-360 | interior |
| Thr359Met (cn210) (refs. 27, 82) | 0.68 | 7/2 | His-348(X) Thr-350(X) | Phe-328, His-348, Thr-350, Val-380 | interior |
| Trp364Cys (cn215) (ref. 27) | 0.73 | 22/4 | Val-376(X) | Thr-239, Ser-320, Pro-321, Met-327, Gly-375, Val-376 | interior |

C_α deviations (Å) were calculated for predicted zymogen structure after aligning the SP domain with the coordinates of the X-ray crystal structure of Banner et al. Surface accessibilities (SA, Å²) are given for both the zymogen and the X-ray crystal structure of Banner et al.³³ H-bonds and the neighbor contacts are evaluated for the zymogen. X denotes the H-bonds also found in the X-ray crystal structure. Residues that form more than one H-bond are in bold.

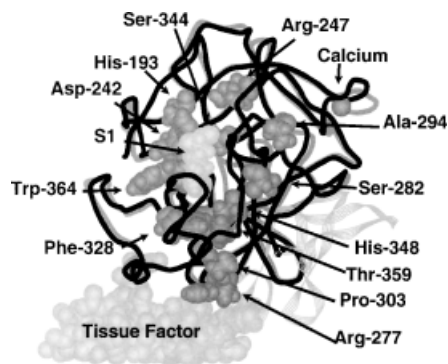


Figure 9. Residues found to be mutated in FVII-deficient patients with severe clinical features. The backbone traces are shown for zymogen (dark) and TF-bound FVIIa of Banner et al.³³ (light). Catalytic triad residues (His-193, Asp-242, and Ser-344) and the SP domain-bound calcium ion are also shown. A TF segment that contacts the FVIIa SP domain is in the bottom left corner. The S1 site is traced by the Arg residue of the inhibitor bound to the FVIIa/TF complex of Banner et al.³³ The backbone ribbon of the EGF2 domain is also shown.

Correlation between Patient Mutation Data and Structure

There are 238 individuals listed in a regularly updated FVII mutation database maintained by the Hemostasis Research group of medical research council of Imperial College, London, UK.⁷⁶ Also, the recent report by McVey et al.⁴ updating mutations serves as an excellent review for the function and characteristics of FVII. There are 70 unique mutations. According to various clinical features, the individuals with identified mutations in FVII were classified as severe, mild, and asymptomatic. Mutations were identified throughout the gene, F7 and affect all domains. A few mutations (detected in the SP domain residues) selected for the present discussion display severe clinical features such as life-threatening mucous membrane, gastrointestinal, and central nervous system bleeding.

In Table 1, we have listed selected severe mutations detected in the SP domain. The domain structures were superimposed for the zymogen and the X-ray crystal structure of Banner et al.³³ Deviations of α -carbons (after the optimal alignment), solvent accessibilities, H-bonds, and the neighbors were evaluated to study the properties and the local environment of these residues to better understand the structural consequences of the reported mutations. The residues that resulted in severe bleeding (once mutated) are shown in Figure 9, along with the three catalytic triad residues and the SP domain-bound calcium ion. Mutations (not included in Table 1) at Arg-152(cn15 mutated to Gln)⁷⁷ and Asp-242(cn102 mutated to His)²⁸ observed in the SP domain must be devastating because the former P1 residue is the key residue in FVII activation and the latter is a member of the catalytic triad that is important in the SP activity.

Two surface residue mutations Arg-277(cn134 mutated to Cys)²⁷ and Pro-303(cn161 mutated to Thr)²⁷ are near the TF-contacting region. In the X-ray crystal structure of Banner et al.,³³ Arg-277(cn134) is found to be in direct contact with TF. Arg-277(cn134) forms a strong H-bond (in both zymogen and X-ray structures) with Arg-304(cn162). The latter residue is located next to Met-306(cn164),^{17, 18, 33} a residue that is TF-inserted in the

TF-bound form of FVIIa. Also, the Arg-304(vn162)Gln mutation results in dysfunctional FVIIa.⁷⁸ Pro-303(cn161), which is located in the second loop segment that interacts with TF, has direct van der Waals contacts with Arg-277(cn134). This residue is in contact with *loop 1* in the previously mentioned “activation domain.”⁷⁴ These observations combined with the unchanged solvent accessibilities and relatively small C_{α} deviations for surface residues lead us to conclude that these residues may participate in the TF-mediated allosteric effect^{18, 79} of FVII activation. With the exception of Arg-247(cn107) and Ala-294(cn152), the remaining mutation residues are located between TF and the catalytic triad or near the S1 specific site. Trp-364(cn215) is in the S1 binding pocket while making direct contact with immediate neighbors of *loop 2* residues in the “activation domain.” There is a strong H-bond between this residue and Val-376(cn227). Phe-328(cn181), His-348(cn199), and Thr-359(cn210) are in close contact with each other. The former two residues maintain direct contact with Arg-304(cn162) mentioned above. Also, His-348(cn199) and Thr-359(cn210) maintain a strong H-bond in both zymogen and TF-bound activated forms. This segment of residues may reasonably be considered an extension of the network that contributes to the allosteric TF-activation of FVII.

Conclusions

We have used MD simulations to estimate the solution structure of zymogen FVII in the absence of TF. The light-chain domain structures (Gla, EGF1, and EGF2) are found to be similar to the corresponding domains of the FVIIa/TF complex of the X-ray crystal form. The properties of the Gla and EGF1 domains that we find in the present simulation for the complete zymogen are similar to those reported previously from the simulation of only the light chain.

We observe significant Gla–EGF1 and EGF1–EGF2 interdomain motion in the present simulation. The active site residues are found to have moved 7 Å away from the hypothetical phospholipid membrane surface when compared with the positions of active sites of TF-bound FVIIa. Thus, we can conclude that a major function of TF binding is to localize FVIIa in a position suitable for its enzyme activity.

The carbohydrate units bound to the EGF1 domain do not interfere with the structural integrity of that domain. Other than the covalent link to the serine residues, the carbohydrate units are free from forming direct interactions with other residues of FVII. Also, they are found to be highly surface exposed and do not compete with the space that is occupied by TF.

The EGF2 domain maintains structural integrity that is likely required for substrate binding. Noticeably, the motif consisting of the strongly H-bonded residues Asn-95, Gln-100, and His-115 is highly conserved during the entire trajectory. Also, we observe minimal interdomain movement associated with the EGF2 and SP domains.

The predicted solution structure of the SP domain is compared with the available X-ray crystal structures determined at different conditions. No major restructuring for this domain is observed either due to activation or due to TF binding. Importantly, the H-bonded network of the catalytic triad is preserved but extended.

The S1 binding site is occupied by Lys-341(cn192) in the predicted zymogen structure. These two factors lead us to conclude that the zymogen FVII also has a pre-formed catalytic triad, and removal of the blocking residues may result in activation. The role of TF for the allosteric interaction between the FVIIa active site and the EGF1 domain is further clarified.

Acknowledgments

We acknowledge Prof. Darrel Stafford at UNC for many useful discussions, and Mr. Vance Shaffer at IBM for assistance. We extend our thanks to the North Carolina Supercomputing Center, the National Cancer Institute, and the Pittsburgh Supercomputing Center for providing required computational resources. Thanks are due to anonymous reviewers for their valuable comments.

Note

A 2.0 Å X-ray crystal structure of the zymogen EGF2-SP domains appeared after our manuscript was accepted. Please see Eigenbrot, C.; Kirchhofer, D.; Dennis, M. S.; Santell, L.; Lazarus, R. A.; Stamos, J.; Ultsch, M. H. *Structure* 2001, 9, 627.

References

- Tuddenham, E. G. *Haemostasis* 1996, 26(Suppl 1), 20.
- Banner, D. W. *Thromb Haemost* 1997, 78, 512.
- Higashi, S.; Iwanaga, S. *Int J Hematol* 1998, 67, 229.
- McVey, J. H.; Boswell, E.; Mumford, A. D.; Kember-Cook, G.; Tuddenham, E. G. *Hum Mutat* 2001, 17, 3.
- Kumar, A.; Fair, D. S. *Eur J Biochem* 1993, 217, 509.
- Petersen, L. C.; Valentin, S.; Hedner, U. *Thromb Res* 1995, 79, 1.
- Nemerson, Y. *Haemostasis* 1996, 26, 98.
- Butenas, S.; Mann, K. G. *Biochemistry* 1996, 35, 1904.
- Persson, E. *Blood Coagul Fibrinolysis* 2000, 11, S15.
- Hagen, F. S.; Gray, C. L.; O'Hara, P.; Grant, F. J.; Saari, G. C.; Woodbury, R. G.; Hart, C. E.; Insley, M.; Kisiel, W.; Kurachi, K. *Proc Natl Acad Sci USA* 1986, 83, 2412.
- Nemerson, Y. *Blood* 1988, 71, 1.
- Lawson, J. H.; Mann, K. G. *J Biol Chem* 1991, 266, 11317.
- Krishnaswamy, S. *J Biol Chem* 1992, 267, 23696.
- Kirchhofer, D.; Nemerson, Y. *Curr Opin Biotechnol* 1996, 7, 386.
- Davie, E. W. *Thromb Haemost* 1995, 74, 1.
- Rapaport, S. I.; Rao, L. V. *Thromb Haemost* 1995, 74, 7.
- Dickinson, C. D.; Kelly, C. R.; Ruf, W. 1996, 93, 14379.
- Dickinson, C. D.; Ruf, W. *J Biol Chem* 1997, 272, 19875.
- Pedersen, A. H.; Lund-Hansen, T.; Bisgaard-Frantzen, H.; Olsen, F.; Petersen, L. C. *Biochemistry* 1989, 28, 9331.
- Nakagaki, T.; Foster, D. C.; Berkner, K. L.; Kisiel, W. *Biochemistry* 1991, 30, 10819.
- Neuenschwander, P. F.; Fiore, M. M.; Morrissey, J. H. *J Biol Chem* 1993, 268, 21489.
- Meade, T. W. *Haemostasis* 1983, 13, 178.
- Triplett, D. A.; Brandt, J. T.; Batard, M. A.; Dixon, J. L.; Fair, D. S. *Blood* 1985, 66, 1284.
- Tuddenham, E. G. D.; Cooper, D. N. *The Molecular Genetics of Haemostasis and Its Inherited Disorder*; Oxford University Press: New York, 1994.
- Tuddenham, E. G.; Pemberton, S.; Cooper, D. N. *Thromb Haemost* 1995, 74, 313.
- Millar, D. S.; Kember-Cook, G.; McVey, J. H.; Tuddenham, E. G.; Mumford, A. D.; Attock, G. B.; Reverter, J. C.; Lanir, N.; Parapia, L. A.; Reynaud, J.; Meili, E.; von Felton, A.; Martinowitz, U.; Prangnell, D. R.; Krawczak, M.; Cooper, D. N. *Hum Genet* 2000, 107, 327.
- Peyvandi, F.; Jenkins, P. V.; Mannucci, P. M.; Billio, A.; Zeinali, S.; Perkins, S. J.; Perry, D. J. *Thromb Haemost* 2000, 84, 250.
- Wulff, K.; Herrmann, F. H. *Hum Mutat* 2000, 15, 489.
- Petersen, L. C.; Hedner, U.; Wildgoose, P. In *Molecular Basis of Thrombosis and Hemostasis*; High, K. A.; Roberts, H. R., Eds.; Marcel Dekker Inc.: New York, 1995.
- Colman, R. W., et al., Eds. *Hemostasis and Thrombosis: Basic Principles and Clinical Practice*; Lippincott: Philadelphia, 1993.
- Kirchhofer, D.; Guha, A.; Nemerson, Y.; Konigsberg, W. H.; Vilbois, F.; Chene, C.; Banner, D. W.; D'Arcy, A. *Proteins* 1995, 22, 419.
- Banner, D. W.; D'Arcy, A.; Chene, C.; Vilbois, F.; Konigsberg, W. H.; Guha, A.; Nemerson, Y.; Kirchhofer, D. *Thromb Haemost* 1995, 73, 1183.
- Banner, D. W.; D'Arcy, A.; Chene, C.; Winkler, F. K.; Guha, A.; Konigsberg, W. H.; Nemerson, Y.; Kirchhofer, D. *Nature* 1996, 380, 41.
- Dennis, M. S.; Eigenbrot, C.; Skelton, N. J.; Ultsch, M. H.; Santell, L.; Dwyer, M. A.; O'Connell, M. P.; Lazarus, R. A. *Nature* 2000, 404, 465.
- Ashton, A. W.; Boehm, M. K.; Johnson, D. J.; Kember-Cook, G.; Perkins, S. J. *Biochemistry* 1998, 37, 8208.
- Kember-Cook, G.; Johnson, D. J.; Tuddenham, E. G.; Harlos, K. *J Struct Biol* 1999, 127, 213.
- Pike, A. C.; Brzozowski, A. M.; Roberts, S. M.; Olsen, O. H.; Persson, E. *Proc Natl Acad Sci USA* 1999, 96, 8925.
- Zhang, E.; St. Charles, R.; Tulinsky, A. *J Mol Biol* 1999, 285, 2089.
- Hamaguchi, N.; Charifson, P.; Darden, T.; Xiao, L.; Padmanabhan, K.; Tulinsky, A.; Hiskey, R.; Pedersen, L. *Biochemistry* 1992, 31, 8840.
- Li, L.; Darden, T. A.; Freedman, S. J.; Furie, B. C.; Furie, B.; Baleja, J. D.; Smith, H.; Hiskey, R. G.; Pedersen, L. G. *Biochemistry* 1997, 36, 2132.
- Perera, L.; Li, L.; Darden, T.; Monroe, D. M.; Pedersen, L. G. *Biophys J* 1997, 73, 1847.
- Perera, L.; Darden, T.; Pedersen, L. G. *Biophys J* 1998, 77, 99.
- Cornell, W. D.; Cieplak, P.; Bayly, C. I.; Gould, I. R.; Merz, K. M., Jr.; Ferguson, D. M.; Spellmeyer, D. C.; Fox, T.; Caldwell, J. W.; Kollman, P. A. *J Am Chem Soc* 1995, 117, 5179.
- Woods, R. J.; Dwek, R. A.; Edge, C. J.; Fraser-Reid, B. *J Phys Chem* 1995, 99, 3832.
- Frisch, M. J.; Trucks, G. W.; Schlegel, H. B.; Scuseria, G. E.; Robb, M. A.; Cheeseman, J. R.; Zakrzewski, V. G.; Montgomery, J. A.; Stratmann, R. E.; Burant, J. C.; Dapprich, S.; Millam, J. M.; Daniels, A. D.; Kudin, K. N.; Strain, M. C.; Farkas, O.; Tomasi, J.; Barone, V.; Cossi, M.; Cammi, R.; Mennucci, B.; Pomelli, C.; Adamo, C.; Clifford, S.; Ochterski, J.; Petersson, G. A.; Ayala, P. Y.; Cui, Q.; Morokuma, K.; Malick, D. K.; Rabuck, A. D.; Raghavachari, K.; Foresman, J. B.; Cioslowski, J.; Ortiz, J. V.; Stefanov, B. B.; Liu, G.; Liashenko, A.; Piskorz, P.; Komaromi, I.; Gomperts, R.; Martin, R. L.; Fox, D. J.; Keith, T.; Al-Laham, M. A.; Peng, C. Y.; Nanayakkara, A.; Gonzalez, C.; Challacombe, M.; Gill, P. M. W.; Johnson, B. G.; Chen, W.; Wong, M. W.; Andres, J. L.; Head-Gordon, M.; Replogle, E. S.; Pople, J. A. *Gaussian 98 (Revision A.7)*; Gaussian Inc.: Pittsburgh, PA, 1998.
- Bayly, C. I.; Cieplak, P.; Cornell, W. D.; Kollman, P. A. *J Phys Chem* 1993, 97, 10269.

47. Jorgensen, W. L.; Chandreskhar, J.; Madura, J. D.; Impey, R. W.; Klein, M. L. *J Chem Phys* 1982, 79, 926.
48. Perera, L.; Foley, C.; Darden, T. A.; Stafford, D.; Mather, T.; Esmon, C. T.; Pedersen, L. G. *Biophys J* 2000, 79, 2925.
49. Essmann, U.; Perera, L.; Berkowitz, M. L.; Darden, T.; Lee, H.; Pedersen, L. G. *J Chem Phys* 1995, 103, 8577.
50. Pearlman, D. A.; Case, D. A.; Caldwell, J. W.; Ross, W. S.; Cheatham, T. E., III; Ferguson, D. M.; Seibel, G. L.; Singh, U. C.; Weiner, P. A.; Kollman, P. A. *Amber 5.0*; University of California, San Francisco, 1995.
51. Harvey, S. C.; Tan, R. K. Z.; Cheatham, T. E., III *J Comp Chem* 1998, 18, 726.
52. Laskowski, R. A.; MacArthur, M. W.; Moss, D. S.; Thornton, J. M. *J Appl Crystallogr* 1993, 26, 283.
53. Martin, D. M.; O'Brien, D. P.; Tuddenham, E. G.; Byfield, P. G. *Biochemistry* 1993, 32, 13949.
54. Nishimura, H.; Kawabata, S.; Kisiel, W.; Hase, S.; Ikenaka, T.; Takao, T.; Shimonishi, Y.; Iwanaga, S. *J Biol Chem* 1989, 264, 20320.
55. Iino, M.; Foster, D. C.; Kisiel, W. *Arch Biochem Biophys* 1998, 352, 182.
56. Kao, Y. H.; Lee, G. F.; Wang, Y.; Starovasnik, M. A.; Kelley, R. F.; Spellman, M. W.; Lerner, L. *Biochemistry* 1999, 38, 7097.
57. Muranyi, A.; Finn, B. E.; Gippert, G. P.; Forsen, S.; Stenflo, J.; Drakenberg, T. *Biochemistry* 1998, 37, 10605.
58. Perera, L.; Darden, T.; Pedersen, L. *Thromb Haemost* 2001, 85, 596.
59. Freskgard, P. O.; Petersen, L. C.; Gabriel, D. A.; Li, X.; Persson, E. *Biochemistry* 1998, 37, 7203.
60. Kavlie, A.; Orning, L.; Grindflek, A.; Stormorken, H.; Prydz, H. *Thromb Haemost* 1998, 79, 1136.
61. Kembball-Cook, G.; Johnson, D. J.; Takamiya, O.; Banner, D. W.; McVey, J. H.; Tuddenham, E. G. *J Biol Chem* 1998, 273, 8516.
62. Hunault, M.; Arbini, A. A.; Carew, J. A.; Peyvandi, F.; Bauer, K. A. *Blood* 1999, 93, 1237.
63. Orning, L.; Stephens, R. W.; Petersen, L. B.; Hamers, M. J.; Stormorken, H.; Sakariassen, K. S. *Thromb Res* 1997, 86, 57.
64. McCallum, C. D.; Hapak, R. C.; Neuenschwander, P. F.; Morrissey, J. H.; Johnson, A. E. *J Biol Chem* 1996, 271, 28168.
65. McCallum, C. D.; Su, B.; Neuenschwander, P. F.; Morrissey, J. H.; Johnson, A. E. *J Biol Chem* 1997, 272, 30160.
66. Hubbard, S. J.; Thornton, J. M. "NACCESS," Computer Program, Department of Biochemistry and Molecular Biology, University College, London, 1993.
67. Kirchhofer, D.; Banner, D. W. *Trends Cardiovasc Med* 1997, 7, 316.
68. Ruf, W.; Dickinson, C. D. *Trends Cardiovasc Med* 1998, 8, 350.
69. Petrovan, R. J.; Ruf, W. *Biochemistry* 2000, 39, 14457.
70. Schiodt, J.; Harrit, N.; Christensen, U.; Petersen, L. C. *FEBS Lett* 1992, 306, 265.
71. Sabharwal, A. K.; Birktoft, J. J.; Gorka, J.; Wildgoose, P.; Petersen, L. C.; Bajaj, S. P. *J Biol Chem* 1995, 270, 15523.
72. Nicholls, A.; Bharadwaj, R.; Honig, B. *Biophys J* 1993, 64, A166.
73. Jin, J.; Perera, L.; Stafford, D.; Pedersen, L. *J Mol Biol* 2001, 98, 5146.
74. Huber, R.; Bode, W. *Acc Chem Res* 1978, 11, 114.
75. Hedstrom, L.; Szilagy, L.; Rutter, W. J. *Science* 1992, 255, 1249.
76. FVII mutation database; <http://192.60.222.13/index.html>.
77. Chaing, S.; Clarke, B.; Sridhara, S.; Chu, K.; Friedman, P.; anDusen, W.; Roberts, H. R.; Blajchman, M.; Monroe, D. M.; High, K. A. *Blood* 1994, 83, 3524.
78. James, H. L.; Girolami, A.; Hubbard, J. G.; Kumar, A.; Fair, D. S. *Biochim Biophys Acta* 1993, 1172, 301.
79. Leonard, B. J.; Clarke, B. J.; Sridhara, S.; Kelley, R.; Ofosu, F. A.; Blajchman, M. A. *J Biol Chem* 2000, 275, 34894.
80. Bhardwaj, D.; Iino, M.; Kontoyianni, M.; Smith, K. J.; Foster, C. D.; Kisiel, W. *J Biol Chem* 1996, 271, 30685.
81. Katsumi, A.; Matsushita, T.; Yamazaki, T.; Sugiura, I.; Kojima, T.; Saito, H. *Thromb Haemost* 2000, 83, 239.
82. Arbini, A. A.; Mannucci, P. M.; Bauer, K. A. *Blood* 1996, 87, 5085.